AIP | Applied Physics Letters

Electrical four-point probing of spherical metallic thin films coated onto micron sized polymer particles

Sigurd R. Pettersen, August Emil Stokkeland, Helge Kristiansen, John Njagi, Keith Redford, Dan V. Goia, Zhiliang Zhang, and Jianying He

Citation: Applied Physics Letters **109**, 043103 (2016); doi: 10.1063/1.4959783
View online: http://dx.doi.org/10.1063/1.4959783
View Table of Contents: http://scitation.aip.org/content/aip/journal/apl/109/4?ver=pdfcov
Published by the AIP Publishing

Electrical four-point probing of spherical metallic thin films coated onto micron sized polymer particles

Sigurd R. Pettersen,[1,a)] August Emil Stokkeland,[1] Helge Kristiansen,[1,2] John Njagi,[3] Keith Redford,[2] Dan V. Goia,[3] Zhiliang Zhang,[1] and Jianying He[1,a)]
[1]*NTNU Nanomechanical Lab, Department of Structural Engineering, Norwegian University of Science and Technology (NTNU), NO-7491 Trondheim, Norway*
[2]*Conpart AS, Dragonveien 54, NO-2013 Skjetten, Norway*
[3]*Center for Advanced Materials Processing, Clarkson University, Potsdam, New York 13699-5814, USA*

(Received 23 May 2016; accepted 7 July 2016; published online 25 July 2016)

Micron-sized metal-coated polymer spheres are frequently used as filler particles in conductive composites for electronic interconnects. However, the intrinsic electrical resistivity of the spherical thin films has not been attainable due to deficiency in methods that eliminate the effect of contact resistance. In this work, a four-point probing method using vacuum compatible piezo-actuated micro robots was developed to directly investigate the electric properties of individual silver-coated spheres under real-time observation in a scanning electron microscope. Poly(methyl methacrylate) spheres with a diameter of 30 μm and four different film thicknesses (270 nm, 150 nm, 100 nm, and 60 nm) were investigated. By multiplying the experimental results with geometrical correction factors obtained using finite element models, the resistivities of the thin films were estimated for the four thicknesses. These were higher than the resistivity of bulk silver. *Published by AIP Publishing*. [http://dx.doi.org/10.1063/1.4959783]

Metal-coated micron-sized polymer spheres (MPS) have long been used as conductive fillers in anisotropic conductive adhesives/films (ACA/ACF) for electronic interconnects,[1] and have recently been presented as a promising alternative to silver flakes in isotropic conductive adhesives (ICAs).[2] The conductivity of these composite materials stems from electrical contacts between the metal films of the particles and the interfaces of the electronic joint. The isotropic conductivity of ICAs is due to inter-particle contacts caused by a much larger volume fraction of particles than that of ACAs.

The bulk electrical resistivity of a conductive composite with a uniform cross-sectional area is easily estimated from the measured bulk resistance, but the electrical properties of the individual filler particles are difficult to investigate. In an ACA assembly wherein individual particles are compressed between the chip and substrate, contact resistance to the contact pads contributes significantly to the measured resistance. Several models have been made to estimate the contact resistances and bulk resistivities of both ACA assemblies[1] and high filler fraction conductive composites,[3] but these all require that the intrinsic resistivity of the conductive filler material is given. The intrinsic resistivity of a flat metallic thin film may deviate from that of the bulk metal. Scattering of electrons at the film surface will become significant as the film thickness approaches the electron mean free path length (EMFP) of the bulk metal,[4] which for silver is 52 nm.[5] If the grain sizes of polycrystalline films are in the same range as the EMFP, electron scattering at the grain boundaries will occur more frequently and increase the resistivity.[6,7] Higher surface roughness in the films will increase the scattering of electrons and can increase film resistivity further.[8] Higher level of impurities[9] and increased porosity[10] may also raise the resistivity, and especially for chemically deposited films, these factors may be a concern. Although these effects occur also in spherical thin films, methods for investigating this have been lacking.

Four-point measurements is a well-known method for investigating the resistivity of flat thin films,[11] but have not been reported for measurements on spherical shell structures such as the metallic thin films of MPS. In this work, four-point measurements were performed directly on individual silver-coated polymer spheres (AgPS) using four separately controlled piezo-actuated micro robots (miBot™ BT-11-VP on a miBase BS-43-VP stage, Imina Technologies, Switzerland), equipped with sharp tungsten (W) probes and connected to an Agilent B2909A Precision Source/Measure Unit (SMU). These micro robots have recently been used to simultaneously apply bending tension and voltage across individual silicon microwires,[12] showing their versatility and positioning resolution. Current (I) was sourced between the outer pair of probes (*source* probes), and the voltage drop (U) along the surface due to resistance in the film was picked up by the inner pair of probes (*sense* probes). The measurements were conducted in a dual beam focused ion beam/scanning electron microscope (FIB/SEM) instrument (FEI Helios NanoLab DualBeam), wherein SEM was used to monitor the movement of the probes in real time. More details can be found in our previous study,[13] as well as in the supplementary material. To provide repeatable apparent contact areas for the probes and decrease the current density at the *source* contacts, the end of the probes were milled to a flat punch geometry approximately 2.5 μm in diameter using FIB. AgPS comprised of poly(methyl methacrylate) (PMMA) spheres with a nominal diameter of 30 μm and nominal silver film thicknesses of 60 nm, 100 nm, 150 nm,

a)Authors to whom correspondence should be addressed. Electronic addresses: sigurd.r.pettersen@ntnu.no and jianying.he@ntnu.no

and 270 nm were provided by Mosaic Solutions AS (Skjetten, Norway). The silver films were coated onto the polymer cores by electroless plating, and the nominal film thicknesses were estimated from the amount of silver used in the plating process. Seven consecutive bi-directional four-point voltage sweeps (0 V → −0.2 mV → 0.2 mV → 0 V) were performed on each measured particle without moving the miBots and an average linear U/I slope was calculated for each measured particle. To compare the real film thicknesses with the nominal values, cross-sections were made with FIB at an incident angle normal to the film surface. Crystallographic data of the silver films were acquired with a Bruker-AXS D8 Focus X-ray diffractometer (XRD). The crystallite sizes were estimated using Scherrer's equation.[14]

In the four-point procedure, the current density is higher closer to the *source* probes, setting up an inhomogeneous electrical field with a distribution dependent on the *source* probe positions. The voltage drop picked up by the *sense* probes is dependent on the positions of the *sense* probes in the field, and the corresponding U/I value is thus a function of all four probe positions. The electrical resistivity of the film is estimated by multiplying the measured U/I value with a correction factor that accounts for specimen shape and probe positions.[11] In this work, the positioning of the probes could be accurately controlled by the miBots with a step-size <100 nm, but there were still variations in probe positions from particle to particle, so a geometric correction factor had to be calculated separately for each measured AgPS. Analytical solutions would only be possible if the *source* probes were placed exactly 180° apart. Finite element (FE) simulations were therefore conducted using the Electric Current (ec) interface of the AC/DC module of COMSOL Multiphysics 5.0. For each measured AgPS, probe positions relative to particle size were acquired from the SEM images and translated into the model using a parameterized geometry and spherical coordinates. Each AgPS-model was built as a homogeneous, fully spherical shell with thickness equal to the nominal film thickness. The probes were simulated as the top surface areas of spherical caps, with sizes approximated from the SEM images. A static voltage field was applied by setting the *source* probes as equipotential surface terminals with different potentials, and the resulting total current I_{FE} was obtained. U_{FE} was calculated by averaging the scalar voltage values at each of the *sense* probes and taking the difference between these.

The FE model solves a current conservation equation based on Ohm's law with the scalar electric potential as the dependent variable. The calculated U/I_{FE} value is thus proportional to the input resistivity value (ρ_{FE}) of the homogeneous shell, and for any specific geometry, the ratio between these will be constant. For a given set of probe positions, U/I_{FE} is independent of the diameter of the shell. Increasing the size of the shell with a factor increases the arc lengths between the probes by the same factor as long as the areas of the probes are increased accordingly. However, this also increases the cross-sectional area of the shell by the same factor, and U/I_{FE} thus remains constant. In contrast, U/I_{FE} is dependent on t^{-1}, where t is the thickness of the shell. The ratio between ρ_{FE} and U/I_{FE} is thus dependent only on three variables: probe positions, the size of the probe areas relative to the surface area of the shell, and shell thickness. This ratio then serves as a geometric correction factor, to which the measured U/I_{miBots} can be multiplied to achieve an estimated film resistivity ρ_{film}

$$\rho_{film} = U/I_{miBots}\frac{\rho_{FE}}{U/I_{FE}}. \quad (1)$$

As can be observed in Fig. 1(a), the positioning control of the miBots is so sensitive that four probes can be placed on a single AgPS without penetrating the thin silver film. Fig. 1(b) shows the seven consecutive voltage sweeps performed on the AgPS in Fig. 1(a). The plots are linear, as expected from measurements on an Ohmic material, and deviations between the measurements are negligible. By linear regression, this particular AgPS yields an average slope (U/I_{miBots}) of 0.126 Ω. The FE model with probe positions acquired from the SEM image in Fig. 1(a) and a shell thickness of 150 nm generates a geometric correction factor of 30.79 nm. Through (1), ρ_{film} is thus estimated as 3.88 μΩ cm for this AgPS. The behavior shown for this particular AgPS is representative for all AgPS measured in this work; each individual AgPS yields linear U/I plots and ρ_{film} higher than that of bulk silver at room temperature, as can be observed in Table I.

U/I_{miBots} follows the expected trend for the 270 nm, 150 nm, and 60 nm films, but the 100 nm films yields lower

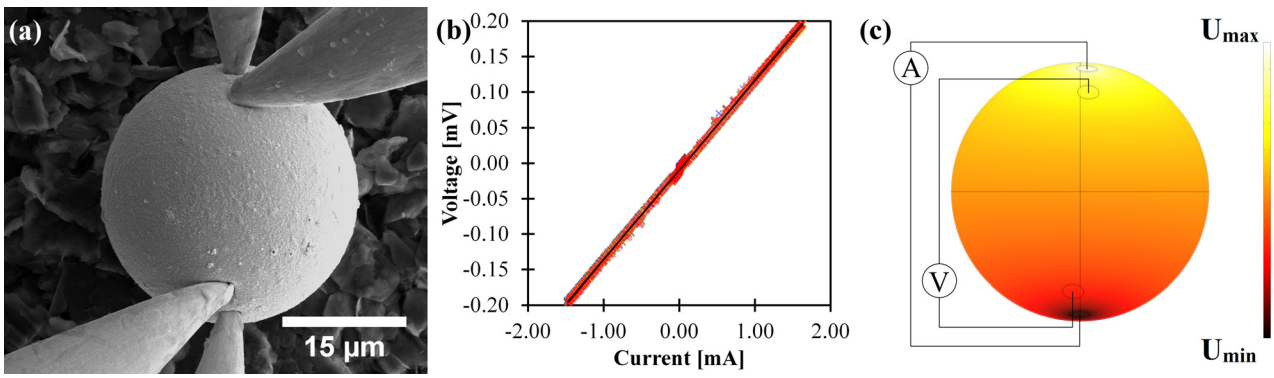

FIG. 1. (a) Four-point probing of a single 30 μm polymer sphere coated with 150 nm silver. (b) Seven consecutive voltage sweeps (0 V → −0.2 mV → 0.2 mV → 0 V) performed on the same particle. (c) The corresponding FE model, showing the voltage field on a 150 nm thick spherical shell with the same probe positions as (a). (The ampere- and volt-meter symbols are included for illustrative purposes.)

TABLE I. Averages ± one standard deviation: U/I_{miBots}, arc lengths along the AgPS surface between *source* probe centers, arc lengths between the *sense* probe centers, and estimated film resistivities. All values are calculated separately for each AgPS and then averaged. For reference, the resistivity of bulk silver at 298 K is 1.62 μΩ cm.[15]

Nominal film thickness (nm)[a]	U/I_{miBots} (Ω)	*Source* arc length (μm)	*Sense* arc length (μm)	ρ_{film} (μΩ cm)
60 ($n = 8$)	0.624 ± 0.209	36.6 ± 2.6	26.6 ± 3.1	7.27 ± 2.59
100 ($n = 17$)	0.080 ± 0.026	35.9 ± 6.1	18.4 ± 5.0	2.47 ± 0.57
150 ($n = 17$)	0.108 ± 0.017	36.6 ± 2.9	25.5 ± 2.9	3.28 ± 0.39
270 ($n = 6$)	0.085 ± 0.008	33.5 ± 4.7	24.5 ± 4.7	4.25 ± 0.44

[a]n = number of individual AgPS measured upon.

values than the 150 nm films. This is partly because some of the 100 nm films were used to test the sensitivity to the *sense* probe positions by positioning these closer together. The measured voltage U between the *sense* probes is dependent on the positions of the probes in the electric field, not just the arc length between the probes. However, the *sense* probes were purposefully placed so that the arc lengths were approximately overlapping with the *source* probe arc lengths, with similar distance between the *source* and *sense* probes at both sides. With these precautions, the ratio between the *source* probe and *sense* probe arc lengths will be the dominating influence on the U/I values of films of the same thickness, as seen in Fig. 2. This partly explains why the 100 nm films yield a lower average U/I_{miBots} value than the 150 nm films. Nevertheless, the FE model accounts for factual probe positions, and the estimated ρ_{film} values suggest that the lower U/I_{miBots} values in the 100 nm films are caused by lower resistivities in these films.

Through (1), ρ_{film} inversely correlates with U/I_{FE}. As U/I_{FE} depends on the thickness t of the homogeneous shell in the FE model by t^{-1}, ρ_{film} is linearly dependent on t. An under- or overestimation of the nominal film thickness compared to the real film thickness will thus cause an under- or overestimation of ρ_{film}. To investigate the real film thickness, cross-sections were ion milled in AgPS. These revealed that the real film thickness inclines toward higher values than the nominal, but only in the range of about 10–30 nm, and with some variations between AgPS of the same nominal thickness. The nominal values are therefore reasonable as conservative average estimates for shell thickness in the FE models, although the obtained ρ_{film} values may be slight underestimations. Deviation between the nominal and real film thicknesses is one potential cause for the scatter observed in ρ_{film} for each of the film thicknesses.

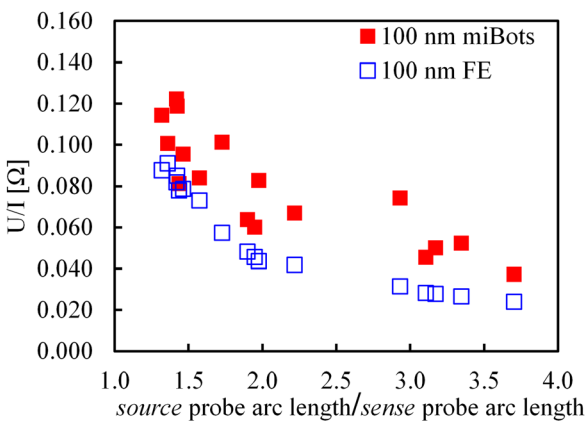

FIG. 2. U/I from miBots measurements and corresponding FE models for each AgPS with 100 nm nominal film thickness. The U/I_{FE} values are calculated with $\rho_{FE} = 1.62$ μΩ cm.

Measurement induced effects, such as probe damage and resistive heating, do not have any observable influence on ρ_{film} (for more details, see the supplementary material). Instead, several factors suggest intrinsic electron scattering effects caused by the structure and compositions of the films. Only the thinnest films have a nominal thickness value at which, for a flat and smooth silver film, we expect the resistivity to be significantly increased due to electron scattering at the surface.[7] However, the surfaces of all four film thicknesses are relatively rough due to the nodular grain structure, which will increase the resistivity compared to smooth films.[8] XRD measurements reveal that the average grain sizes are smaller than the EMFP of bulk silver for all four film thicknesses, as can be observed in Table II. Interestingly, the average grain size of the thickest film is smaller than those of the 150 nm and 100 nm films, almost as small as for the thinnest films. This coincides well with the estimated resistivity values in Table I and suggests that the elevation in resistivity is at least partly caused by increased electron scattering due to shorter distance between grain boundaries.[6,7] Although the four series have the same cores, they were coated separately with slight changes in process parameters to achieve the different film thicknesses, which can cause some variations in film structure. The 100 nm films yield lower resistivities than the 150 nm coatings, while being comprised of smaller grains, suggesting influence also from other scattering mechanisms. As the different film thicknesses were prepared in separate processes, it is possible that the level of impurities varies between the films. Impurities can increase the resistivity either by disrupting the lattice structure inside the grains, or by increasing the grain boundary reflection.[9] Different levels of porosity is also a potential contributing factor behind the differences in ρ_{film}.[10] It may also be that the relative underestimation of film thickness is slightly larger for the 100 nm than the 150 nm films.

TABLE II. Grain sizes calculated from peak with highest intensity in the XRD spectra obtained for the four nominal film thicknesses.

270 nm (nm)	150 nm (nm)	100 nm (nm)	60 nm (nm)
28	44	33	25

We have shown that it is possible to perform four-point measurements directly on spherical thin films coated onto micron-sized polymer particles using micromanipulators with step size resolution in the nanometer range. By multiplying the measured U/I values with geometrical correction factors obtained from simple FE models, probe positions can be accounted for, and the resistivities of the thin films estimated. Spherical electroless plated silver thin films yield higher resistivities than bulk silver at four different thicknesses, which are attributed to higher levels of electron scattering compared to bulk silver. It is evident that simply increasing the amount of silver, i.e., the film thickness, does not necessarily yield better electric properties. To gain efficient usage of the plating metal, it is desirable to control the grain size, as well as keep the porosity and level of impurities at a minimum.

See supplementary material for a more thorough description and discussion of the measurements and FE model, as well as XRD spectra for the four nominal film thicknesses.

The Research Council of Norway is acknowledged for funding through Project No. 225962/E20—"Novel conductive adhesive technology for solar industry" and for the support to the Norwegian Micro- and Nano-Fabrication Facility, NorFab. Partial funding has also been obtained from the European Union Seventh Framework Programme FP7-NMP-2013-LARGE-7 under Grant Agreement No. 604668 ("Quantiheat") and by funding from the European Union Seventh Framework Programme (FP7/2007-2013) under Grant Agreement No. FP7-NMP-310420 ("HyperConnect"). Vidar T. Fauske (Department of Physics, NTNU) is acknowledged for writing the control script for the sourcemeter.

[1]M. Chin, K. A. Iyer, and S. J. Hu, IEEE Trans. Compon. Packag. Technol. **27**, 317 (2004).
[2]J. Gakkestad, P. Dalsjo, H. Kristiansen, R. Johannessen, and M. M. Visser Taklo, J. Micro/Nanolithogr., MEMS, MOEMS **9**, 041108 (2010); S. R. Pettersen, H. Kristiansen, S. Nagao, S. Helland, J. Njagi, K. Suganuma, Z. Zhang, and J. He, J. Electron. Mater. **45**, 3734 (2016).
[3]G. R. Ruschau, S. Yoshikawa, and R. E. Newnham, J. Appl. Phys. **72**, 953 (1992).
[4]K. Fuchs, Math. Proc. Cambridge **34**, 100 (1938); E. H. Sondheimer, Adv. Phys. **1**, 1 (1952).
[5]U. Kreibig and C. v. Fragstein, Z. Phys. **224**, 307 (1969).
[6]A. F. Mayadas and M. Shatzkes, Phys. Rev. B **1**, 1382 (1970).
[7]W. Zhang, S. H. Brongersma, O. Richard, B. Brijs, R. Palmans, L. Froyen, and K. Maex, Microelectron. Eng. **76**, 146 (2004).
[8]S. M. Rossnagel and T. S. Kuan, J. Vac. Sci. Technol., B **22**, 240 (2004); V. J. Logeeswaran, N. P. Kobayashi, M. Saif Islam, W. Wu, P. Chaturvedi, N. X. Fang, S. Y. Wang, and R. S. Williams, Nano Lett. **9**, 178 (2009).
[9]E. E. Glickman, V. Bogush, A. Inberg, Y. Shacham-Diamand, and N. Croitoru, Microelectron. Eng. **70**, 495 (2003).
[10]M. S. M. Peterson and M. Deutsch, J. Appl. Phys. **106**, 063722 (2009).
[11]L. B. Valdes, Proc. IRE **42**, 420 (1954); F. M. Smits, Bell Syst. Tech. J. **37**, 711 (1958).
[12]M. M. McClarty, J. P. Bruce, M. S. Freund, and D. R. Oliver, Appl. Phys. Lett. **106**, 022107 (2015).
[13]A. E. Stokkeland, M.S. thesis, Norwegian University of Science and Technology, 2015.
[14]P. Scherrer, Göttinger Nachrichten Math. Phys. **2**, 98 (1918); available at https://eudml.org/doc/59018.
[15]R. A. Matula, J. Phys. Chem. Ref. Data **8**, 1147 (1979).